Acta Astronautica 177 (2020) 438–445

Contents lists available at ScienceDirect

Acta Astronautica

journal homepage: www.elsevier.com/locate/actaastro

Synthesis and characterization of light-weight porous ceramics used in the transpiration cooling

Bo Zhang [a], Jie Huang [a,b], Weijie Li [a], Haiming Huang [a], Huanyu Zhao [a], Jinlong Peng [c]

[a] Institute of Engineering Mechanics, Beijing Jiaotong University, Beijing, 100044, China
[b] School of Computer and Information Technology, Beijing Jiaotong University, Beijing, 100044, China
[c] Institute of Mechanics, Chinese Academy of Sciences, Beijing, 100190, China

ARTICLE INFO

Keywords:
Carbon fiber-reinforced silicon carbide porous ceramics
Permeability
Oxyacetylene flame test
Transpiration cooling

ABSTRACT

Light-weight carbon fiber-reinforced silicon carbide (C/SiC) porous ceramics have been fabricated by optimized grinding-mould pressing-sintering process, and the properties of the porous ceramics have been discussed systematically. The results demonstrate that fabricated porous ceramics used in the transpiration cooling exhibit low densities (1.327–1.377 g/cm^3), uniform pore-size distribution and excellent permeabilities (5.713–5.903 × 10^{-8} mm^2). Furthermore, the validity and reliability of the porous ceramics applied as coolant medium in the transpiration cooling system are successfully verified by using the oxyacetylene flame test. This work provides an efficient method to prepare light-weight C/SiC porous ceramics with excellent permeability, which has a useful reference for optimization of the transpiration cooling of the hypersonic vehicles.

1. Introduction

Thermal protection system is a key technology for development of hypersonic vehicles [1,2]. As one of the thermal protection methods, transpiration cooling system has a promising potential development for protecting hypersonic vehicles from outside thermal loads due to maintaining the aerodynamic shape of the vehicle [3,4]. Porous material applied as coolant medium plays a key role in this thermal protection system, in which the coolant is fed through this porous material [5–9]. The cooling mechanism mainly relies on the heat capacity of the coolant and external film cooling, which decreases the heat flux of porous material wall from searing gas.

Recently, sintered porous plate [10,11], porous C/C composites [12,13] and sintered woven wire mesh [14,15] are used as coolant medium to investigate the performances of transpiration cooling. However, these porous materials for transpiration cooling are still limited in high density or low application temperature, these shortcomings are detrimental to fuel economy and flight safety for the vehicle.

C/SiC porous ceramic has low density [16–18], prominent high temperature oxidation resistance [19–22] and remarkable mechanical property [23–26], so it is a prospective porous material in the transpiration cooling system. Unfortunately, to the best of our knowledge, few of specialized studies focus on the development of the silicon carbide matrix porous ceramics applied in the transpiration cooling system [27]. Besides, it still has great room for porous ceramic with low density used in the transpiration cooling. In this study, an optimized fabrication method is proposed for C/SiC porous ceramics in the pursuit of low density and excellent permeability, the effects of different impregnation materials on the performances of this porous ceramic are also discussed. Besides, transpiration cooling tests for these porous ceramics prepared in the work are successfully carried out using the oxyacetylene flame test.

2. Experimental procedure

The preparation steps of C/SiC porous ceramics are shown in Fig. 1: firstly, the SiC ceramic slurry is prepared. A percentage of dispersants (Silok-7096, Silok®Chemical group co., Ltd, China; Anjeka 6041, Ezhou anjieka technology co., Ltd, China) and polycarbosilane (PCS, melting point of 200 °C, average molecular weight of 1234, Suzhou saifei group co., Ltd, China) are dissolved in xylene. β-SiC particles (5 μm in diameter) are served as the starting particles in the slurry. Next, carbon fiber powders (7 μm in diameter, 150 μm in diameter, the mass ratio between silicon carbide particles and carbon fiber powders is 1:1) are added into the prepared SiC ceramic slurry to obtain the dried mixture by stirring and drying. After that, the dried mixture is grinded into hybrid powders, and then the hybrid powders are molded at 100 MPa to form black bodies. Subsequently, black bodies are sintered to form initial C/SiC

E-mail address: huanghaiming@tsinghua.org.cn (H. Huang).

https://doi.org/10.1016/j.actaastro.2020.08.008
Received 29 June 2020; Received in revised form 30 July 2020; Accepted 4 August 2020
Available online 10 August 2020

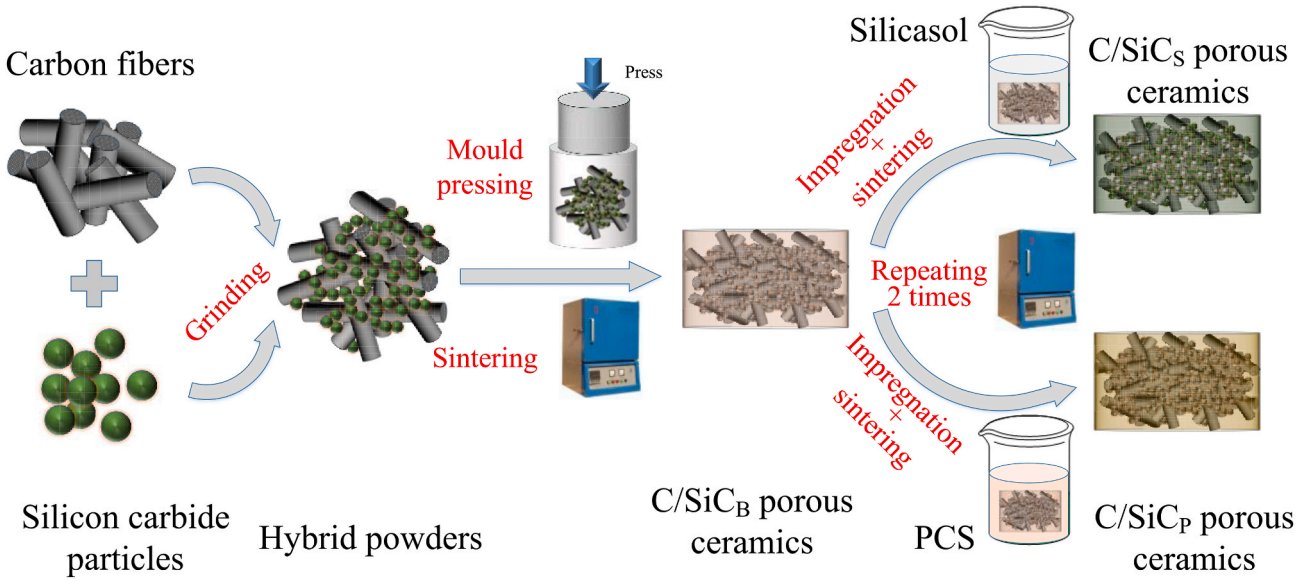

Fig. 1. Preparation flow chart of porous ceramics.

porous ceramics (C/SiC_B porous ceramics for short, these abbreviations of porous ceramics are shown in Table 1) at 1300 °C for 2 h under the protection of nitrogen after crosslinking in the air, followed by natural cooling. Finally, the final C/SiC porous ceramics (C/SiC_P porous ceramics and C/SiC_S porous ceramics, these abbreviations of porous ceramics are shown in Table 1) are respectively prepared by impregnating C/SiC_B porous ceramics with PCS solution (mass fraction of 20%) or silicasol solution (mass fraction of 20%) under vacuum conditions, and sintering at 1300 °C under nitrogen atmosphere after dried. The impregnation process is repeated 2 times. After each impregnation, porous ceramics are dried and sintered.

The microstructures of polished C/SiC porous ceramic samples are observed by scanning electron microscopy. Testing samples with dimensions of 1 cm × 1 cm × 1 cm are cut from the primary samples, whereafter, mechanical strengths of the C/SiC porous ceramics are determined under quasi-static states by using a microcomputer controlled spring tension and compressive testing machine. Densities of C/SiC porous ceramics are based upon mass-to-volume ratio of the samples. Pore-size distributions are analyzed by a mercury intrusion porosimetry. Permeabilities of the porous ceramics are obtained using by a self-made apparatus, which has been detailedly described in Ref. [6]. Transpiration cooling tests for C/SiC porous ceramics are carried out using the oxyacetylene flame test, its schematic diagram is shown in Fig. 2. Oxygen and acetylene are adjusted by the control system to flow through flame gun and then they are ignited to spray to specimen. The temperature sensor and water pipe are installed on the back-side of specimen. The experimental data are saved into the data collection system. The oxyacetylene flame test details have been introduced in Refs. [7].

Table 1
Abbreviations of porous ceramics.

Porous ceramic description	Abbreviation
C/SiC porous ceramics before impregnation	C/SiC_B porous ceramics
C/SiC porous ceramics are impregnated with PCS	C/SiC_P porous ceramics
C/SiC porous ceramics are impregnated with silicasol	C/SiC_S porous ceramics

3. Results and discussion

Light weight is a prerequisite for hypersonic vehicles, so light-weight porous ceramics used in the transpiration cooling have been fabricated by optimized grinding-mould pressing-sintering process and the properties of porous ceramics before and after impregnation have also been investigated in this work. As shown in Fig. 3, the densities and application temperatures of C/SiC porous ceramics in this study and other the transpiration cooling materials have been compared. It is obvious that porous ceramics in this work have higher application temperature and lower density. Fig. 4 displays the micrographs of C/SiC porous ceramics before and after impregnation. It can be obviously noticed that the carbon fiber powders are uniformly dispersed inside the porous ceramics, besides, the porous ceramics before and after impregnation have fluffy structures, which can provide ample space for coolant in the transpiration cooling. Characterizations of porous ceramics are shown in Table 2. After impregnation, the porous ceramics have lower open porosities, but the open porosity is still higher than that of porous ceramic in Refs. [6], and the morphology of porous ceramic after impregnation has no significant change as compared to that before impregnation.

Fig. 5 depicts the stress versus the displacement for C/SiC porous ceramics before and after impregnation. It is clear that different impregnation materials have important impacts on the mechanical performance of this porous ceramic [34–37]. C/SiC_P porous ceramic has the highest mechanical strength, while the stress of untreated porous ceramic is the lowest. As is known to all, the mechanical properties of sintered powder porous ceramics primarily rely on the bonding state among the powders [38,39]. As shown in Fig. 6(a), SiO_2 evenly distributes in the cavity of porous ceramic, but it contributes limited bonding strength. Fig. 6(c) depicts that the carbon thermal reaction

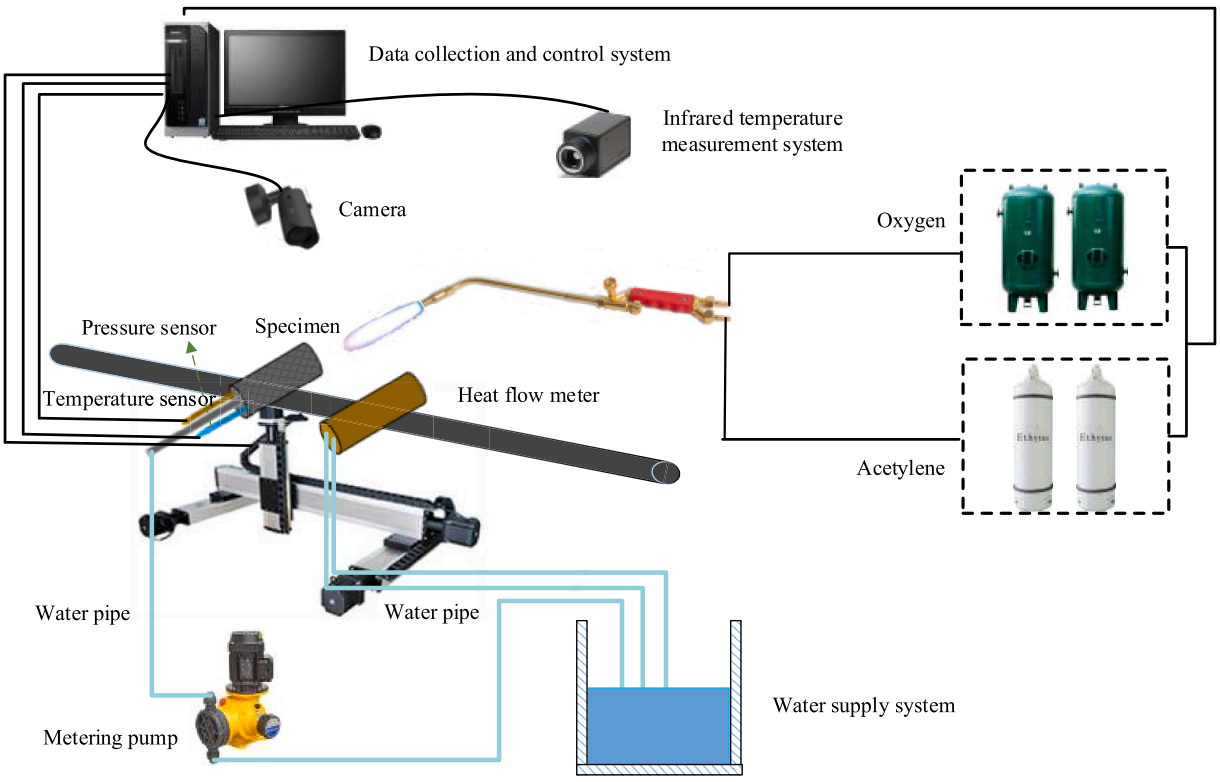

Fig. 2. Schematic diagram of oxyacetylene flame test.

between the C and SiO_2 has occurred, but this reaction cannot completely happen at 1300 °C in Fig. 6(b). Thereby the main reasons for improving mechanical property of C/SiC_S porous ceramic probably include increasing of the compactionness of porous ceramic and the joint area among silicon carbide particles, carbon fibers and SiO_2. As shown in Fig. 6(d) and (e), as the product derived from PCS is same to substrate of porous ceramic, the strength of joints among silicon carbide particles are very strong, and the joints between carbon fiber and silicon carbide particles can also be bonded. Thus, the bonding performance of C/SiC_P porous ceramic is higher than that of C/SiC_S porous ceramic [40,41]. Notably, it is clear that the fracture mechanism of C/SiC porous ceramic before impregnation is ductile failure, while brittle failure is dominant for C/SiC porous ceramic after impregnating silicasol or PCS because of improvement of brittle matrix content [42]. The impregnation-sintering process has a great effect on the mechanical performance of porous ceramic [43,44].

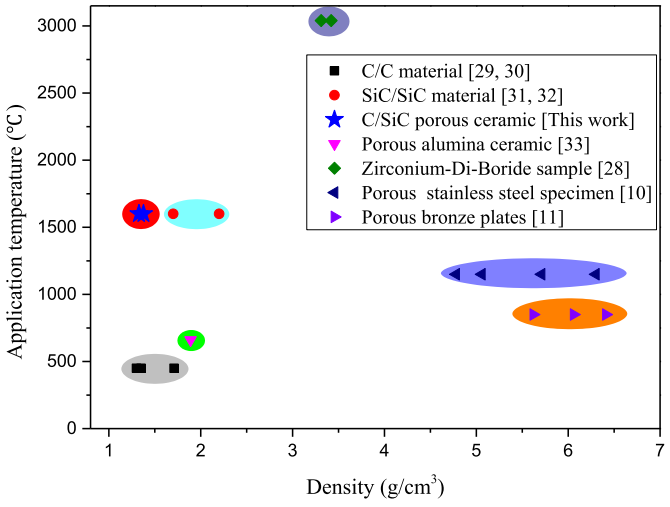

Fig. 3. The densities and application temperatures of the C/SiC porous ceramics are comparable to other transpiration cooling materials [28–33].

In the transpiration cooling process, pore sizes inside porous material should be as uniform as possible to avoid irregular distribution of coolant. Fig. 7 shows pore-size distributions of C/SiC porous ceramics before and after impregnation. It is evident that all pore-size distributions respectively reveal a narrow peak in the range of 2–25 μm. Meanwhile, there are some large-sized pores at 100–300 μm, which are mainly composed of the gaps between the carbon fibers and SiC particles, as shown in Fig. 4(a). Porous ceramics after impregnation have a higher proportion of smaller pores, because silicasol and PCS fill the space of larger pores. These pores can be the channels for coolant, and make the coolant uniformly distribute in the porous ceramics.

It is well known that permeability has always been a prerequisite for coolant medium in the transpiration cooling [45,46]. As is shown in Table 2, C/SiC porous ceramics before and after impregnation all have excellent permeabilities, which are much faster than those of C/SiC porous ceramics in Ref. [6]. The permeability of C/SiC_P porous ceramics has been improved by at least 45% as compared to that of C/SiC porous ceramics fabricated in Ref. [6]. Apart from the driving force from the metering pump in the permeability test (Fig. 2), the capillary force also plays an important role in this porous ceramic, because complete wetting of material is primarily dependent on the capillary driven imbibition of liquid water. The capillary driven imbibition and seepage flow processes in the porous media under microgravity conditions have been investigated experimentally and theoretically in Refs. [47,48], and the

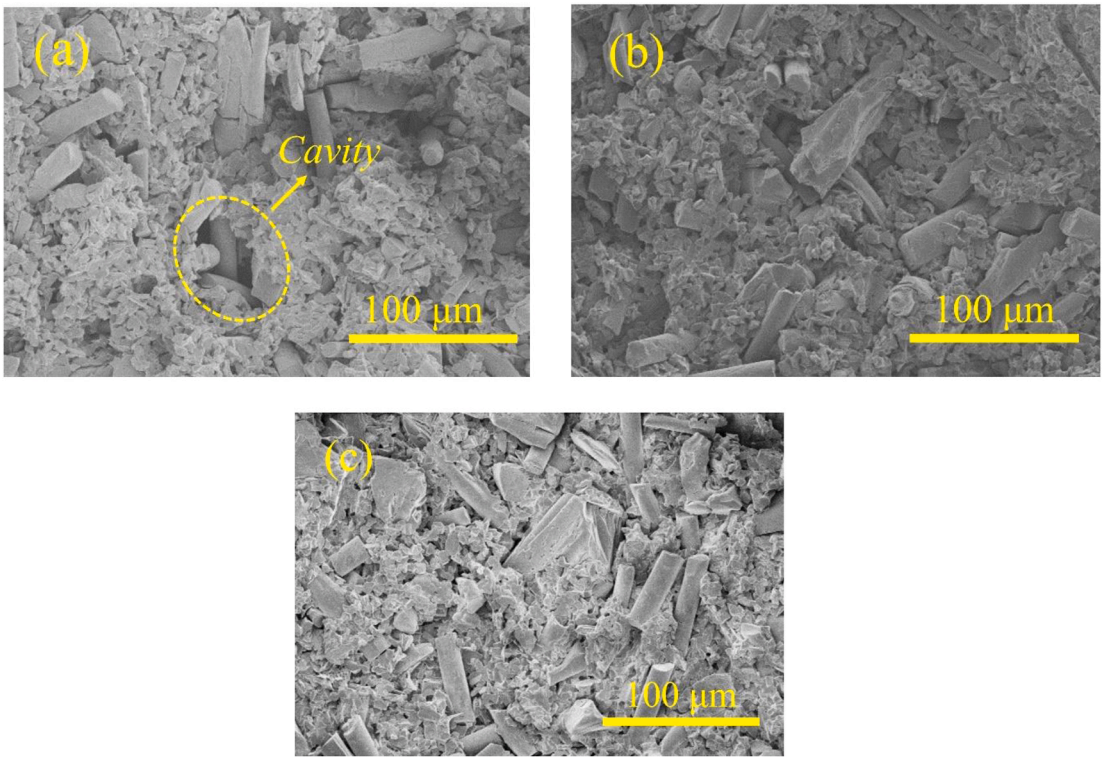

Fig. 4. Micrographs of porous ceramics: (a) C/SiC_B porous ceramics, (b) C/SiC_S porous ceramics, (c) C/SiC_P porous ceramics.

Table 2
Comparison of characterizations of C/SiC porous ceramics before and after impregnation.

Samples porous ceramics	Density (g/cm^3)	Open porosity (%)	Compressive strength (MPa)	Permeability rate ($\times 10^{-8}$ mm^2)
C/SiC_B	1.229 ± 0.055	13.2 ± 1.3	10.36 ± 0.56	7.951 ± 1.102
C/SiC_S	1.327 ± 0.045	10.6 ± 0.5	15.70 ± 0.75	5.903 ± 0.676
C/SiC_P	1.377 ± 0.092	11.2 ± 0.9	23.08 ± 0.328	5.713 ± 0.887

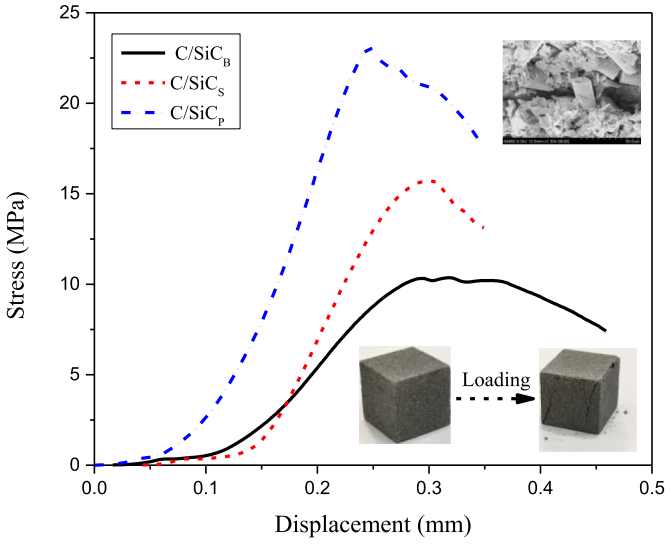

Fig. 5. Stress-displacement curves of porous ceramics before and after impregnation.、

capillary force still has an effect on the seepage flow processes though there is external pressure gradient in the porous media [49]. As shown in Fig. 8, the liquid water has firstly wetted the surface and then evenly seeped out from this porous ceramic under the metering pump and capillary force, which indicates the porous ceramic is hydrophilic, these two driving forces are simultaneous until the porous ceramic is completely filled with water; then, there is no longer capillary force [50, 51].

Several experimental investigations on transpiration cooling of these porous ceramics with water coolant are carried out using the oxyacetylene flame test, and the surface and back-side temperatures of different porous ceramics are shown in Fig. 9. It is apparent that the surface and back-side temperatures have quickly achieved stable states at different heat fluxes in Fig. 9(b), respectively. During about 600-s tests, the back-side temperatures have been stayed at a low level, which indicates that these porous ceramics can be successfully applied in the transpiration cooling system. Fig. 9(a) displays that surface and back-side temperatures of different porous ceramics at heat flux of 1.9 MW/m^2 and liquid water flow rate of 0.06 g/s. The surface temperatures of porous ceramics after impregnation are higher than those of porous ceramics before impregnation, because C/SiC porous ceramics after impregnation have lower porosities, there is less room inside porous ceramic to store water

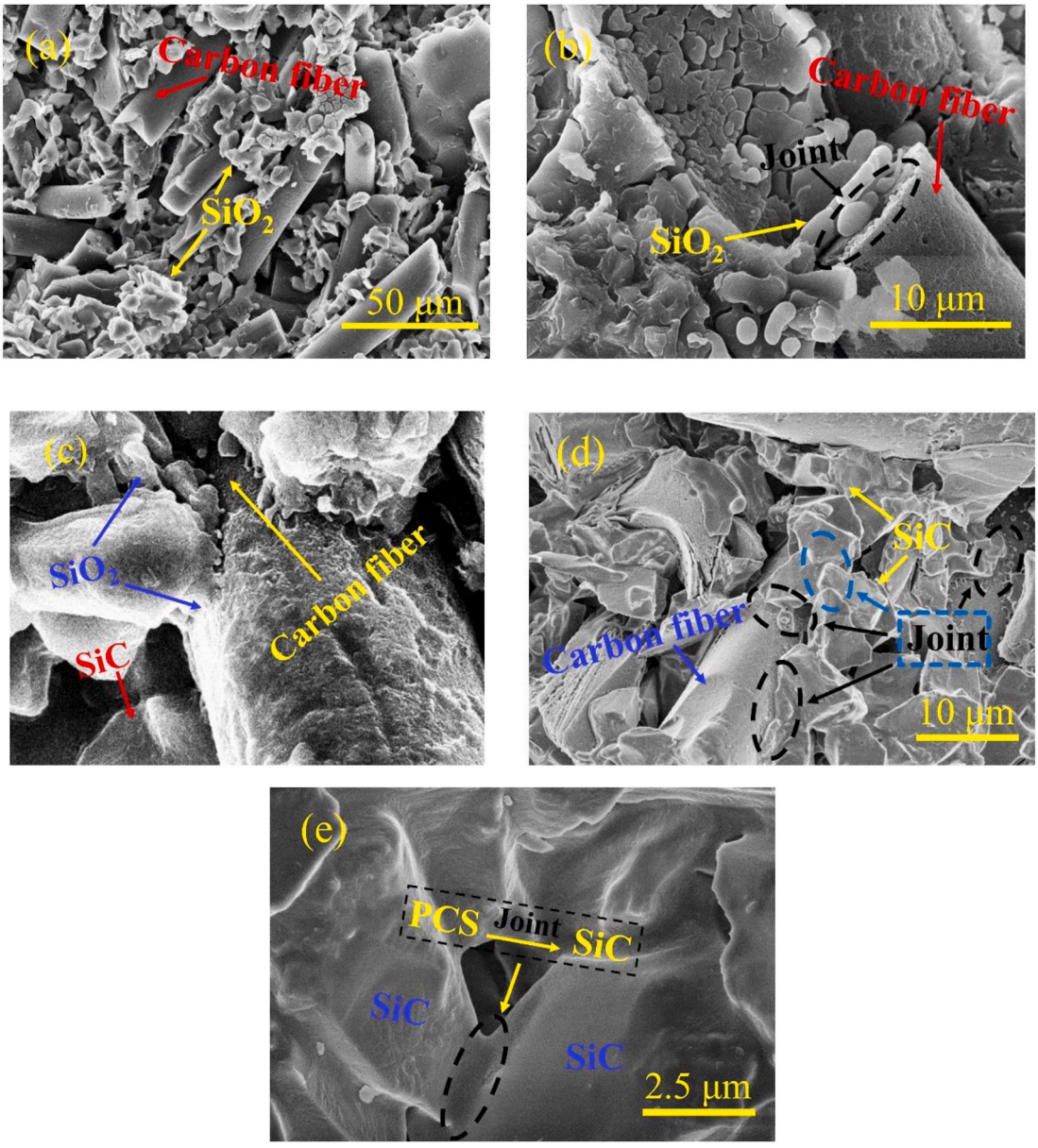

Fig. 6. Bonding state: (a) SEM picture of C/SiC_S porous ceramics; (b) joint between SiO_2 and carbon fiber; (c) joint between SiO_2 and carbon fiber; (d) SEM picture of C/SiC_P porous ceramics; (e) joint between SiC particle and SiC particle of C/SiC_P porous ceramics.

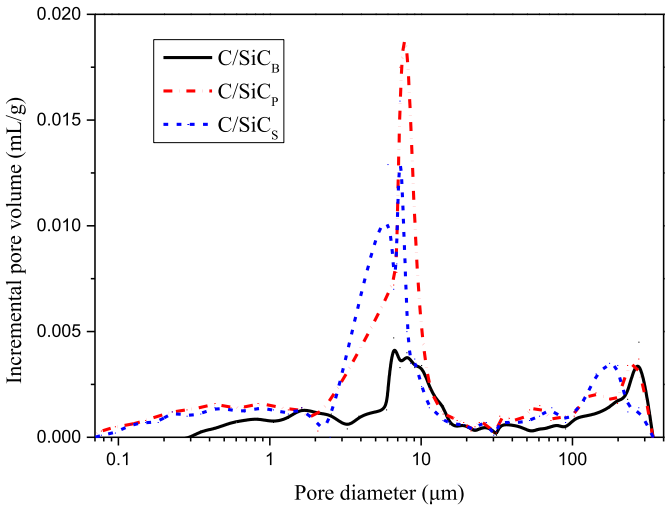

Fig. 7. The pore-size distributions of C/SiC porous ceramics before and after impregnation.

and pore skeletons have smaller heat-exchange area with liquid water. Similarly, the same reason probably causes that surface temperatures of C/SiC$_S$ porous ceramics are higher than those of C/SiC$_P$ porous ceramics. In practical application, the mechanism of transpiration cooling still needs to be systematically studied because the transpiration heat-protection effect is still affected by various factors. As shown in Fig. 9 (b), with the increasing of heat flux, surface and back-side temperatures all gradually increase but back-side temperatures increase more slowly than surface temperatures. These porous ceramics all achieve good cooling effects. After several tests, these porous ceramics perform well at different testing conditions, as is shown in Fig. 10. These results indicate that it is valid and reliable for these porous ceramics applied as coolant medium in the transpiration cooling system of hypersonic vehicles.

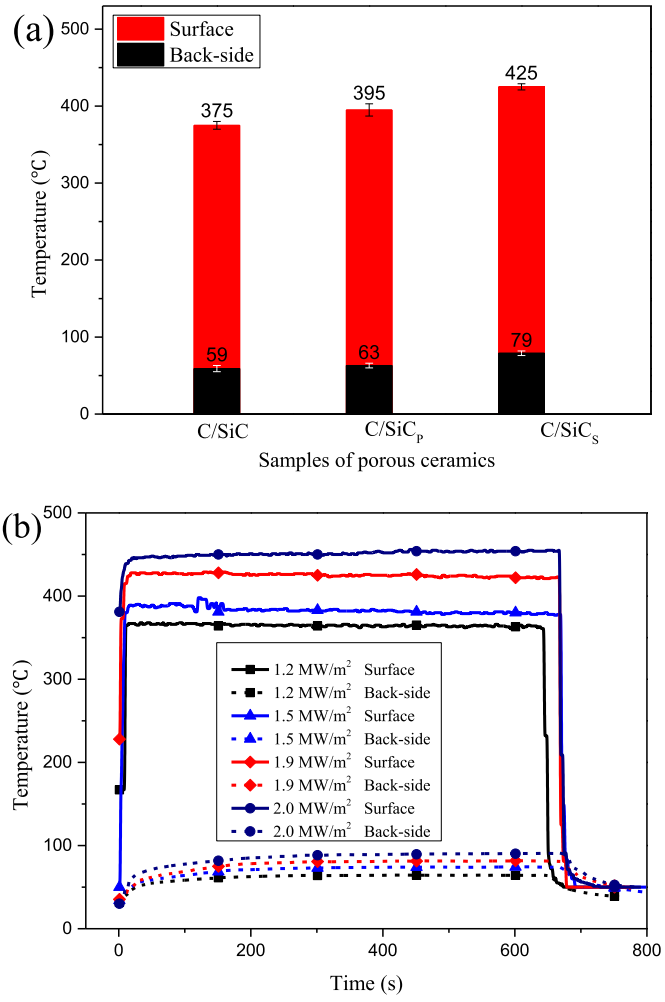

Fig. 9. Surface temperatures: (a) different porous ceramics at heat flux 1.9 MW/m^2, (b) C/SiC$_S$ porous ceramic with different heat fluxes at water rate 0.06 g/s.

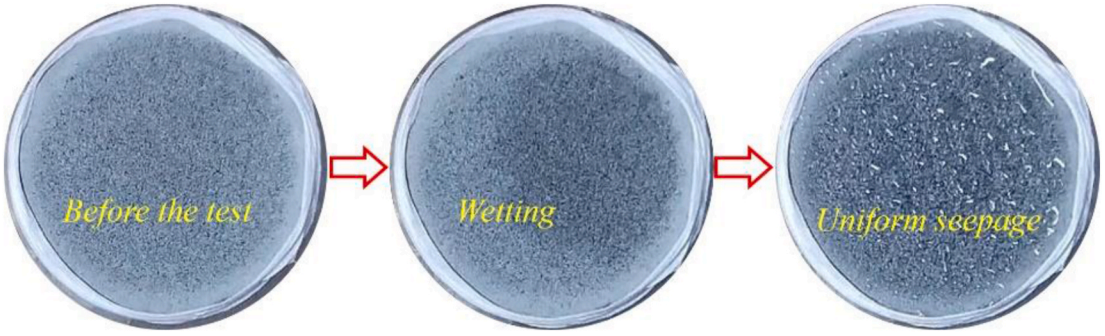

Fig. 8. Permeability test.

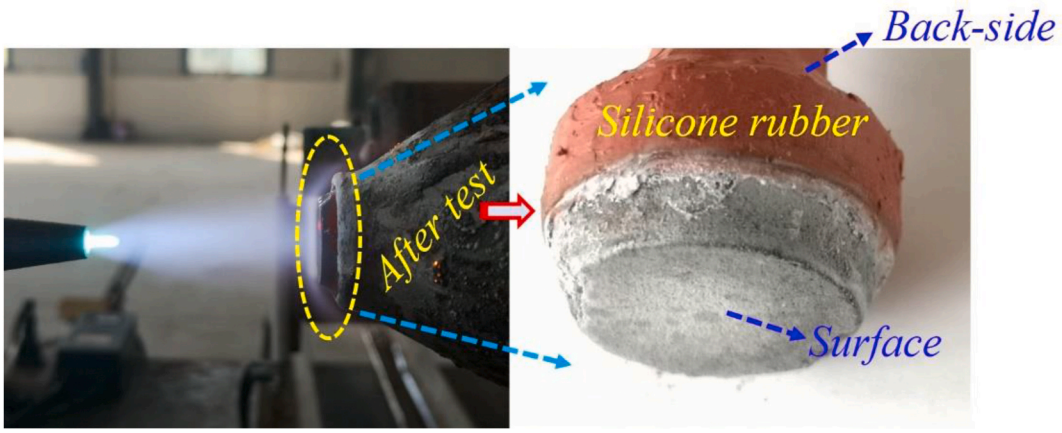

Fig. 10. Cross view of C/SiC_S porous ceramic during and after test.

4. Conclusions

Light-weight carbon fiber-reinforced silicon carbide (C/SiC) porous ceramics are fabricated by optimized grinding-mould pressing-sintering process. The porous ceramics in this work have higher application temperatures and lower densities as compared to other the transpiration cooling materials. The properties of porous ceramics before and after impregnation have been systematically compared and discussed. The mechanical performance of porous ceramic has been reinforced after impregnation, especially mechanical strength of C/SiC porous ceramic after polycarbosilane impregnation. Additionally, the porous ceramic after impregnation has a more uniform pore-size distribution. Moreover, the C/SiC porous ceramic after several tests at high heat flux is performing well and it can be re-used in the transpiration cooling experiments. In summary, porous ceramic after polycarbosilane impregnation has the most superior properties among these three porous ceramics in this work. Therefore, C/SiC porous ceramic after polycarbosilane impregnation in this work have a likely potential application in the transpiration cooling thermal protection system.

Declaration of competing interest

The authors declare that they have no known competing financial interests or personal relationships that could have appeared to influence the work reported in this paper.

Acknowledgements

This work was supported by the Fundamental Research Funds for the Central Universities (Grant No. 2019YJS110).

References

[1] W.J. Li, J. Huang, Z.W. Zhang, H.M. Huang, J. Liang, Competition mechanism during oxidation of pyrolysis gases in nonequilibrium boundary layer on thermal protection performance of charring composites, Polym. Compos. (2020) 1–12, https://doi.org/10.1002/pc.25571.
[2] N.N. Smirnov, V.V. Tyurenkova, M.N. Smirnova, Laminar diffusion flame propagation over thermally destructing material, Acta Astronaut. 109 (2015) 217–224, https://doi.org/10.1016/j.actaastro.2014.09.016.
[3] S. Liu, B.M. Zhang, Experimental study on a transpiration cooling thermal protection system, Sci. China Technol. Sci. 53 (10) (2010) 2765–2771, https://doi.org/10.1007/s11431-010-4055-8.
[4] M. Zheng, G. Huang, S.N. Parbat, L. Yang, M.K. Chyu, Experimental investigation on additively manufactured transpiration and film cooling structures, J. Turbomach. 141 (1–10) (2019), 031009, https://doi.org/10.1115/1.4042009.
[5] N.N. Smirnov, V.F. Nikitin, V.R. Dushin, A. Maximenko, M. Thiercelin, J.C. Legros, Instability in displacement of viscous fluids from porous specimens, Acta Astronaut. 61 (7–8) (2007) 637–643, https://doi.org/10.1016/j.actaastro.2006.12.004.
[6] B. Zhang, H.M. Huang, X.L. Lu, Fabrication and properties of C/SiC porous ceramics by grinding-mould pressing-sintering process, J. Eur. Ceram. Soc. 39 (5) (2019) 1775–1780, https://doi.org/10.1016/j.jeurceramsoc.2019.01.004.
[7] B. Zhang, H.M. Huang, J. Huang, J.L. Chen, An experimental investigation on performance of transpiration cooling with liquid water through C/SiC porous ceramic, Appl. Therm. Eng. 178 (2020) 115526, https://doi.org/10.1016/j.applthermaleng.2020.115526.
[8] M. Ahangarkani, K. Zangeneh-Madar, S. Borji, Transpiration cooling during ultra-high temperature erosion, Mater. Lett. 216 (2018), https://doi.org/10.1016/j.matlet.2017.10.015, 113-113.
[9] S.M. Ibrahim, P. Vivek, K.P.J. Reddy, Experimental investigation on transpiration cooling effectiveness for spacecraft entering martian atmosphere, AIAA J. 54 (2016) 2920–2924, https://doi.org/10.2514/1.J054757.
[10] N. Wu, J.H. Wang, F. He, G.Q. Dong, L.S. Tang, An experimental investigation on transpiration cooling of a nose cone model with a gradient porosity layout, Exp. Therm. Fluid Sci. 106 (2019) 194–201, https://doi.org/10.1016/j.expthermflusci.2019.05.002.
[11] G. Huang, Y.H. Zhu, Z.Y. Liao, X.L. Ouyang, P.X. Jiang, Experimental investigation of transpiration cooling with phase change for sintered porous plates, Int. J. Heat Mass Tran. 114 (2017) 1201–1213, https://doi.org/10.1016/j.ijheatmasstransfer.2017.05.114.
[12] T. Langener, J.V. Wolfersdorf, M. Selzer, H. Hald, Experimental investigations of transpiration cooling applied to C/C material, Int. J. Therm. Sci. 54 (2012) 70–81, https://doi.org/10.1016/j.ijthermalsci.2011.10.018.
[13] S. Gulli, L. Maddalena, Characterization of complex porous structures for reusable thermal protection systems: effective-permeability measurements, J. Spacecraft Rockets 51 (2014) 1943–1953, https://doi.org/10.2514/1.A32980.
[14] J.D. Ma, P. Lv, X. Luo, Y.P. Liu, H.W. Li, J. Wen, Experimental investigation of flow and heat transfer characteristics in double-laminated sintered woven wire mesh, Appl. Therm. Eng. 95 (2016) 53–61, https://doi.org/10.1016/j.applthermaleng.2015.11.015.
[15] G.Q. Xu, Y.P. Liu, X. Luo, J.D. Ma, H.W. Li, Experimental investigation of transpiration cooling for sintered woven wire mesh structures, Int. J. Heat Mass Tran. 91 (2015) 898–907, https://doi.org/10.1016/j.ijheatmasstransfer.2015.07.060.
[16] Z.Y. Zhai, W.J. Wang, J. Zhao, X.S. Mei, K.D. Wang, F.C. Wang, H.Z. Yang, Influence of surface morphology on processing of C/SiC composites via femtosecond laser, Composer Part A-Appl. S. 102 (2017) 117–125, https://doi.org/10.1016/j.compositesa.2017.07.031.
[17] J.H. Shaw, M.N. Rossol, D.B. Marshall, F.W. Zok, Effects of tow-scale holes on the mechanical performance of a 3D woven C/SiC composite, J. Am. Ceram. Soc. 98 (2015) 948–956, https://doi.org/10.1111/jace.13389.
[18] L. Zhang, D.Z. Yin, R.J. He, Z.J. Yu, K.Q. Zhang, Y.F. Chen, X.J. Bai, Y.Z. Yang, D. N. Fang, Lightweight C/SiC ceramic matrix composite structures with high loading capacity, Adv. Eng. Mater. 21 (1–12) (2019) 1801246, https://doi.org/10.1002/adem.201801246.
[19] W. Zhu, H. Fu, Z.F. Xu, R.Z. Liu, P. Jiang, X.Y. Shao, Y.S. Shi, C.Z. Yan, Fabrication and characterization of carbon fiber reinforced SiC ceramic matrix composites based on 3D printing technology, J. Eur. Ceram. Soc. 38 (14) (2018) 4604–4613, https://doi.org/10.1016/j.jeurceramsoc.2018.06.022.
[20] B. Zhang, H.M. Huang, X.L. Lu, X.L. Xu, J. Yao, Fabrication and properties of SiC porous ceramics using a polyurethane preparation process, Ceram. Int. 44 (2018) 16589–16593, https://doi.org/10.1016/j.ceramint.2018.06.083.
[21] X.M. Ren, B.Y. Ma, C. Su, F. Qian, W.G. Yang, L. Yuan, J.K. Yu, G.Q. Liu, H.X. Li, In-situ synthesis of fe_xsi_y phases and their effects on the properties of SiC porous ceramics, J. Alloys Compd. 784 (2019) 1113–1122, https://doi.org/10.1016/j.jallcom.2019.01.031.
[22] Z.J. Wu, Z. Wang, G.D. Shi, J. Sheng, Effect of surface oxidation on thermal shock resistance of the ZrB_2-SiC-ZrC ceramic, Compos. Sci. Technol. 71 (2011) 1501–1506, https://doi.org/10.1016/j.compscitech.2011.06.008.

[23] Y.L. Xia, Z.L. Lu, J.W. Cao, K. Miao, J. Li, D.C. Li, Microstructure and mechanical property of C_f/SiC core/shell composite fabricated by direct ink writing, Scripta Mater. 165 (2019) 84–88, https://doi.org/10.1016/j.scriptamat.2019.02.016.
[24] F. Yang, X.H. Wang, T. Zeng, G.D. Xu, S. Cheng, H.M. Chen, Mechanical property of C/SiC corrugated lattice core composite sandwich panels after high temperature annealing, Compos. Struct. 210 (2019) 687–694, https://doi.org/10.1016/j.compstruct.2018.11.097.
[25] T. Li, J.J. Mo, X. Yu, T. Suo, Y.L. Li, Mechanical behavior of C/SiC composites under hypervelocity impact at different temperatures: micro-structures, damage and mechanisms, Composer Part A-Appl. S. 88 (2016) 19–26, https://doi.org/10.1016/j.compositesa.2016.05.015.
[26] S. Hofmann, B. Ozturk, D. Koch, H. Voggenreiter, Experimental and numerical evaluation of bending and tensile behaviour of carbon-fibre reinforced SiC, Composer Part A-Appl. S. 43 (2012) 1877–1885, https://doi.org/10.1016/j.compositesa.2012.07.017.
[27] B. Zhang, H.M. Huang, X.L. Lu, J.L. Peng, Experimental investigation on transpiration cooling for porous ceramic with liquid water, Acta Astronaut. 167 (2020) 117–121, https://doi.org/10.1016/j.actaastro.2019.11.009.
[28] M.E. Rocher, T. Hermanny, M. McGilvray, H. Saad Ifti, F. Hufgard, M. Eberhartk, A. Meindl, S. Lohle, T. Giovanninizz, L. Vandeperre, Testing a transpiration cooled zirconium-di-boride sample in the plasma tunnel at IRS, AIAA Scitech (2019 Forum), https://doi.org/10.1016/10.2514/6.2019-1552.c1.
[29] M. Ortelt, Dr H. Hald, I. Fischer, D. Greuel, Dr O. Haidn, Dr D. Suslov, Empirical verification of effusion cooled CMC rocket thrust chambers, 41st AIAA/ASME/SAE/ASEE Joint Propulsion Conference & Exhibit (2005), https://doi.org/10.1016/10.2514/6.2005-3569.
[30] H. Hald, A. Herbertz, M. Kuhn, M. Ortelt, Technological aspects of transpiration cooled composite structures for thrust chamber applications, 16th AIAA/DLR/DGLR International Space Planes and Hypersonic Systems and Technologies Conference (2009), https://doi.org/10.2514/6.2009-7222.
[31] T. Hayashi, S. Wakayama, Thermal Fatigue Behavior of 3D-Woven SiC/SiC composite with porous matrix for transpiration cooling passages, Adv. Compos. Mater. 18 (2009) 61–75, https://doi.org/10.1163/156855108X379354.
[32] J. Tang, Y.F. Chen, J.G. Sun, H. Wang, H.L. Liu, Q.C. Fan, Properties and application of oriented porous SiC as transpiration cooling materials, Key Eng. Mater. 336–338 (2007) 1109–1112. https://dx.doi.org/10.4028/www.scientific.net/KEM.336-338.1109.
[33] H. Otsu, K. Fujita, T. Ito, Application of the transpiration cooling method for reentry vehicles, 45th AIAA Aerospace Sciences Meeting and Exhibit, Reno, Nevada (2007), https://doi.org/10.2514/6.2007-1209.
[34] O. Homoro, M. Michel, T.N. Baranger, Pull-out response of glass yarn from ettringite matrix: effect of pre-impregnation and embedded length, Compos. Sci. Technol. 170 (2019) 174–182, https://doi.org/10.1016/j.compscitech.2018.11.045.
[35] B. Zhang, H.M. Huang, X.L. Lu, Fabrication and properties of C/SiO_2 composites by silicasol-impregnation-sintering process, J. Alloys Compd. 789 (2019) 357–361, https://doi.org/10.1016/j.jallcom.2019.03.039.
[36] R. Fu, H.Y. Weng, J.F. Wenk, A. Martin, Thermomechanical coupling for charring ablators, J. Thermophys. Heat Tran. 32 (2) (2018) 369–379, https://doi.org/10.2514/1.T5194.
[37] R. Venugopalan, M. Roy, S. Thomas, A.K. Patra, D. Sathiyamoorthy, A.K. Tyagi, Effect of impregnation pressure and time on the porosity, structure and properties of polyacrylonitrile-fiber based carbon composites, J. Nucl. Mater. 433 (2013) 494–503, https://doi.org/10.1016/j.jnucmat.2012.10.017.
[38] V. Iacobellis, A. Radhi, K. Behdinan, Discrete element model for ZrB_2-SiC ceramic composite sintering, Compos. Struct. 229 (2019) 111373, https://doi.org/10.1016/j.compstruct.2019.111373.
[39] T. Whitiow, J. Pitz, J. Pierce, S. Hawkins, A. Samuel, K. Kollins, G. Jefferson, E. Jones, J. Vernon, C. Przybyla, Thermal-mechanical behavior of a SiC/SiC CMC subjected to laser heating, Compos. Struct. 210 (2019) 179–188, https://doi.org/10.1016/j.compstruct.2018.11.046.
[40] H.Q. Ly, R. Taylor, R.J. Day, F. Heatley, Conversion of polycarbosilane (PCS) to SiC-based ceramic - Part 1. Characterisation of PCS and curing products, J. Mater. Sci. 36 (2001) 4037–4043, https://doi.org/10.1023/A:1017942826657.
[41] J.H. Lee, Y. Lee, Y.H. Han, D.G. Shin, S. Kim, B.K. Jang, Microstructural studies of core/rim structure of polycarbosilane-derived SiC consolidated by spark plasma sintering, Ceram. Int. 45 (2019) 12406–12410, https://doi.org/10.1016/j.ceramint.2019.03.171.
[42] H.M. Li, B.M. Zhang, G.H. Bai, Effects of constructing different unit cells on predicting composite viscoelastic properties, Compos. Struct. 125 (2015) 459–466, https://doi.org/10.1016/j.compstruct.2015.02.028.
[43] Y. Zhang, L.T. Zhang, J.X. Zhang, X.W. Yin, C.D. Liu, Effects of z-pin's porosity on shear properties of 2D C/SiC z-pinned joint, Compos. Struct. 173 (2017) 106–114, https://doi.org/10.1016/j.compstruct.2017.04.013.
[44] T.K. Ye, Y.X. Xu, J. Ren, Effects of SiC particle size on mechanical properties of SiC particle reinforced aluminum metal matrix composite, Mat. Sci. Eng. A-Struct. 753 (2019) 146–155, https://doi.org/10.1016/j.msea.2019.03.037.
[45] H. Najmi, N. Gascoin, K. Chetehouna, E. El-Tabach, S. Akridiss, Transient and spatial evolution of clogging of porous material by filtrating particles, Ind. Eng. Chem. Res. 58 (2019) 12261–12271, https://doi.org/10.1021/acs.iecr.9b01746.
[46] G. Fantozzi, M. Kinell, S.R. Carrera, J. Nilsson, Y. Kuesters, Experimental study on pressure losses in porous materials, J. Eng. Gas Turbines Power 141 (2019), https://doi.org/10.1115/1.4040868. GTP-18-1349.
[47] N.N. Smirnov, J.C. Legros, V.F. Nikitin, E. Istasse, L. Schramm, F. Wassmuth, D'Arcy Hart, Filtration in artificial porous media and natural sands under microgravity conditions, Microgravity Sci. Technol. 14 (2) (2003) 3–28, https://doi.org/10.1007/BF02870312.
[48] N.N. Smirnov, V.F. Nikitin, J.C. Legros, E. Istasse, L. Schramm, F. Wassmuth, Microgravity investigations of capillary-driven imbibition and drainage in inhomogeneous porous media, Acta Astronaut. 54 (2003) 39–52, https://doi.org/10.1016/S0094-5765(02)00278-3.
[49] V.R. Dushin, V.F. Nikitin, N.N. Smirnov, E.I. Skryleva, V.V. Tyurenkova, Microgravity investigation of capillary driven imbibition, Microgravity Sci. Technol. 30 (2018) 393–398, https://doi.org/10.1007/s12217-018-9623-8.
[50] K. Okada, S. Uchiyama, T. Isobe, Y. Kameshima, A. Nakajima, T. Kurata, Capillary rise properties of porous mullite ceramics prepared by an extrusion method using organic fibers as the pore former, J. Eur. Ceram. Soc. 29 (2009) 2491–2497, https://doi.org/10.1016/j.jeurceramsoc.2009.03.012.
[51] N.N. Smirnov, V.F. Nikitin, E.I. Skryleva, Microgravity investigation of seepage flows in porous media, Microgravity Sci. Technol. 31 (2019) 629–639, https://doi.org/10.1007/s12217-019-09733-7.